

# Electronic structure, donor and acceptor transitions, and magnetism of 3d impurities in $\text{In}_2\text{O}_3$ and ZnO

Hannes Raebiger,\* Stephan Lany, and Alex Zunger

National Renewable Energy Laboratory, Golden, Colorado 80401, USA

(Received 16 December 2008; revised manuscript received 21 February 2009; published 8 April 2009)

3d transition impurities in wide-gap oxides may function as donor/acceptor defects to modify carrier concentrations, and as magnetic elements to induce collective magnetism. Previous first-principles calculations have been crippled by the LDA error, where the occupation of the 3d-induced levels is incorrect due to spurious charge spilling into the misrepresented host conduction band, and have only considered magnetism and carrier doping separately. We employ a band-structure-corrected theory, and present simultaneously the chemical trends for electronic properties, carrier doping, and magnetism along the series of  $3d^1$ – $3d^8$  transition-metal impurities in the representative wide-gap oxide hosts  $\text{In}_2\text{O}_3$  and ZnO. We find that most 3d impurities in  $\text{In}_2\text{O}_3$  are amphoteric, whereas in ZnO, the early 3d's (Sc, Ti, and V) are shallow donors, and only the late 3d's (Co and Ni) have acceptor transitions. Long-range ferromagnetic interactions emerge due to partial filling of 3d resonances inside the conduction band and, in general, require electron doping from additional sources.

DOI: 10.1103/PhysRevB.79.165202

PACS number(s): 75.50.-y, 85.75.-d

## I. INTRODUCTION

The deep 3d levels in Si, III-V, and II-VI semiconductors were reviewed already three decades ago (see Refs. 1–4), as was traditional interest in wide-gap oxides.<sup>5–8</sup> This interest has recently been rekindled<sup>9</sup> because of three developments: (i) advances in making and understanding dopable transparent conductors for photovoltaics and flat-panel displays,<sup>9</sup> (ii) the emergence of ferromagnetic (FM) semiconductors for spintronics,<sup>10–12</sup> and (iii) the potential of using doped oxides as agents for photoelectrochemical water splitting.<sup>13,14</sup> Here, we focus on tuning such properties of wide-gap oxides, via doping by 3d transition-metal elements.

3d impurities in semiconductors and oxides manifest interesting and diverse phenomenology. They often induce deep gap levels<sup>1–4</sup> that exist in multiple charged configurations,<sup>4,15,16</sup> thus having multiple (donor/acceptor) transitions within the band gap. Considering dopable transparent conductors, intentional extrinsic defects, together with intrinsic impurities, govern the conductivity and transparency of the host semiconductor. The ensuing Fermi level and *n*-type, *p*-type, or nonconductive behavior are determined by the thermodynamic interplay of all defects involved,<sup>17,18</sup> and the thermodynamic Fermi level in turn determines the electronic configuration of the transition-metal defect, related to a nominal oxidation state.<sup>16</sup> Considering spintronic applications, the different oxidation states of the 3d impurities correspond to different spin configurations, and if the defect has a magnetic moment, it may give rise to collective magnetism. Despite this obvious link between electronic (spin) configuration and the ensuing defect (acceptor/donor) levels,<sup>16</sup> this link remains poorly established.

A major reason for the missing quantitative description of transition-metal impurity levels in wide-gap oxides is the failure of conventional local-density calculations to correctly predict these levels relative to the host band edges, due to the dramatic underestimation of the conduction-band energies in, e.g., ZnO or  $\text{In}_2\text{O}_3$ .<sup>19,20</sup> We here remedy this problem by employing simultaneously a band-gap correction via nonlo-

cal external potentials<sup>19</sup> and on-site Coulomb energy corrections<sup>21</sup> for the transition-metal impurities.

To understand the coexistence of transparency, conductivity, and ferromagnetism, we calculate the spin configuration, ensuing defect levels, and donor/acceptor transition energies of a series of 3d transition element defects in both ZnO and  $\text{In}_2\text{O}_3$  host materials. We consider transition elements from  $3d^1$  to  $3d^8$ , that is, Sc to Ni in ZnO, and Ti to Cu in  $\text{In}_2\text{O}_3$ . Understanding the electronic spin configuration allows us to evaluate the donor/acceptor transition energies and the magnetization of each defect. These donor/acceptor transition energies allow us to evaluate carrier densities, i.e., conductive properties, and further calculation of 3d-3d magnetic coupling energies allows us to evaluate the possibilities for collective magnetism.

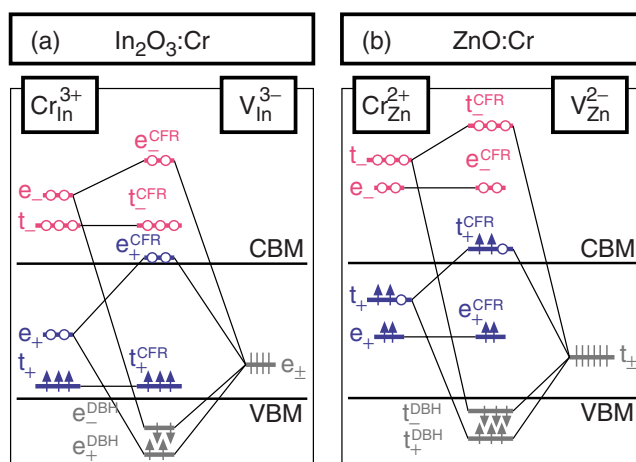


FIG. 1. (Color online) Formation of 3d defect levels for Cr substituting a host cation in (a)  $\text{In}_2\text{O}_3$  and (b) ZnO. The Cr *d* orbital splits into crystal-field levels with *t* and *e* representations, which interact with dangling-bond states of the cation vacancy with the same representation. Notice that due to the lower oxidation state of Cr in ZnO than in  $\text{In}_2\text{O}_3$ , the Cr levels are higher in energy in ZnO.

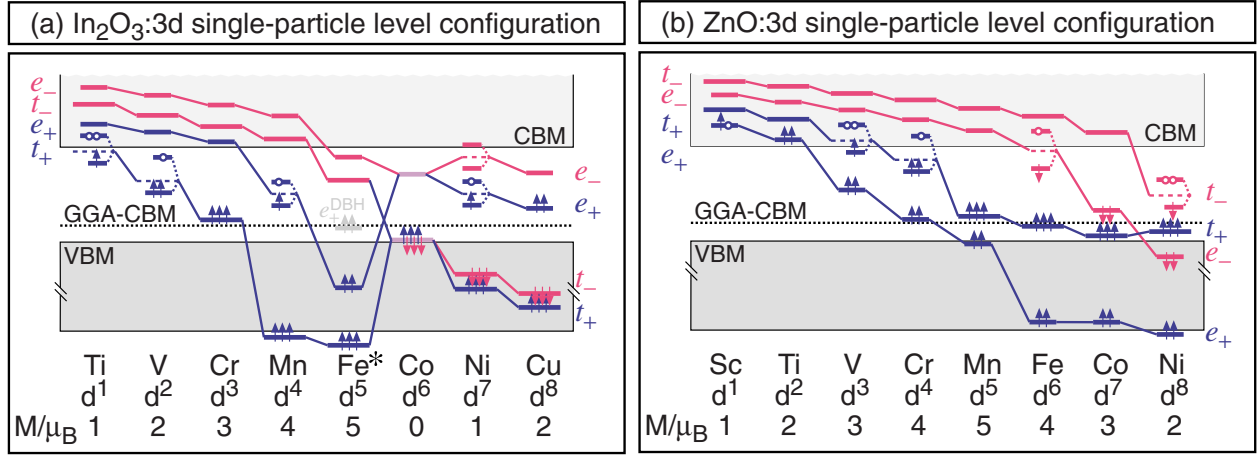


FIG. 2. (Color online) Schematic diagram of single-particle levels (spin configuration) for charge neutral 3d impurities in (a)  $\text{In}_2\text{O}_3$  and (b)  $\text{ZnO}$ . We only show the “crystal-field resonances” (CFRs) (see Fig. 1), except for the Fe in  $\text{In}_2\text{O}_3$  (denoted by an asterisk), where both majority-spin crystal-field resonances are below the valence-band minimum, and there is a dangling-bond hybrid (DBH) level in the gap.

## II. TERMINOLOGY

We describe the electronic structure obtained from density-functional calculations in terms of “single-particle levels,” formed by the Kohn-Sham eigenvalues. These single-particle levels are then explained in terms of simple band models (Figs. 1 and 2), and are not to be confused with donor/acceptor “transition levels”  $\varepsilon(q/q')$  (Fig. 3), which describe the threshold energy to convert the system from “charge state”  $q$  to  $q'$ . Such a charge state  $q$  simply denotes a specific occupancy of the aforementioned single-particle Kohn-Sham levels, and  $\varepsilon(q/q')$  in essence describes the transition of an electron from the valence continuum to a defect level (acceptor), or from a defect level to the conduction continuum of states (donor). We make a clear distinction between these different (albeit related) quantities by calling  $\varepsilon(q/q')$  “transition energies,” and restricting “level” to the Kohn-Sham single-particle levels.

## III. METHODS

We calculate the electronic configurations of the  $3d^1$ – $3d^8$  impurities Sc to Ni in  $\text{ZnO}$  and Ti to Cu in  $\text{In}_2\text{O}_3$  by replacing one cation with the respective 3d element in a supercell

of 72 and 80 host atoms for  $\text{ZnO}$  and  $\text{In}_2\text{O}_3$ , respectively. The electronic structure is then calculated using the projector-augmented wave method<sup>22</sup> within a host band-structure-corrected density functional.<sup>19</sup> Using the self-consistent band-structure correction, we avoid the spurious charge spilling from occupied 3d impurity levels into unoccupied host crystal conduction states, as described in Refs. 19 and 20. In essence, the host band structure is corrected by shifting the conduction band upward using a repulsive (non-local) potential acting on the cation  $s$  states. To obtain overall agreement with experimental and  $\text{GW}$ -calculated band structures, small attractive potentials  $V_{T,\ell}$  are added on cation  $p$  and anion  $s$  and  $p$  states, together with the on-site Coulomb correction  $U_{T,d}$  on  $d$  states for each atom type  $T$ . The potential parameters, summarized in Table I, are empirically determined<sup>19,20</sup> such as to fit multiple band-structure properties taken from experiment<sup>23,24</sup> and  $\text{GW}$  calculations.<sup>25</sup> For the transition metal impurities, on-site Coulomb corrections  $U_{T,d}$  (tabulated in Table II), determined such as to reproduce the thermochemical stability of different oxide stoichiometries (e.g., NiO vs  $\text{Ni}_2\text{O}_3$ ; see Refs. 26 and 27), are applied on the  $d$  states together with  $J=1.0$  eV. The present values for  $U$  were obtained with the LDA+ $U$  formulation of Ref. 21(b). Supercell size effects have been treated as described in

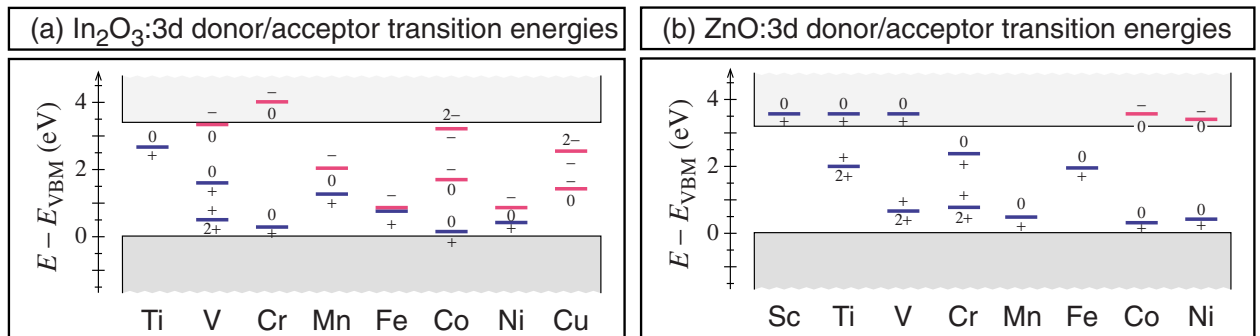


FIG. 3. (Color online) Donor and acceptor transition energies for 3d impurities in (a)  $\text{In}_2\text{O}_3$  and (b)  $\text{ZnO}$ . Donor and acceptor transitions are denoted by blue and red lines, respectively. The charge states  $q$  below and above the transition energy are denoted below and above the line. The energies are given with respect to the host valence-band maximum.

TABLE I. Potential parameters (in eV) for host band-structure correction.

Host	$V_{\text{Zn}/\text{In } s}$	$V_{\text{Zn}/\text{In } p}$	$V_{\text{O } s}$	$V_{\text{O } p}$	$U_{\text{Zn}/\text{In } d}$
ZnO	9.4	-1.2	-6.4	-2.0	7.0
$\text{In}_2\text{O}_3$	10.5	0	-6.4	-2.0	5.5

Refs. 28 and 29. In particular, we showed in Ref. 29 that finite-size effects for charged defects are effectively eliminated when the 3rd order image charge interaction and potential alignment effects are taken into account simultaneously. Remarkably, the full 3rd order image charge correction can be accurately approximated by a simple scaling factor for the 1st order (screened) Madelung term.<sup>29</sup> Here we include also image charge terms for shallow states that act similarly to a compensating background.<sup>29,30</sup>

#### IV. ELECTRONIC AND SPIN CONFIGURATIONS OF SINGLE IMPURITIES

Before presenting the detailed results, we discuss the level formation in terms of a simple energy-level model (Fig. 1). The defect levels can be understood to be the result of coupling between the levels of the host cation vacancy (anion dangling bonds) and the symmetry-adapted 3d orbitals of the impurity. In  $\text{In}_2\text{O}_3$  there are two inequivalent cation sites, both of which can be approximated by the octahedral symmetry, and in  $\text{ZnO}$  the cation site is tetrahedral. The symmetry-adapted 3d levels split into crystal-field levels with  $e$  and  $t$  representations. In the octahedral symmetry of the  $\text{In}_2\text{O}_3$  cation site, the doubly degenerate  $e$  level interacts with host dangling-bond states, and in the tetrahedral  $\text{ZnO}$  cation site, the triply degenerate  $t$  level interacts with host dangling-bond states, forming hybrid levels, as shown in Fig. 1 and discussed, e.g., in Ref. 16. Thus, for  $\text{In}_2\text{O}_3:3d$ , upon cation substitution in the octahedral In site, two hybrid  $e$  levels and one nonbonding  $t$  level are formed. For  $\text{ZnO}:3d$ , in the tetrahedral Zn site, two hybrid  $t$  levels and a nonbonding  $e$  level are formed. Notice that, even though the valence and conduction bands of  $\text{ZnO}$  and  $\text{In}_2\text{O}_3$  are close in energy,<sup>31</sup> the single-particle levels of Cr (or any other particular transition element) are higher in energy in  $\text{ZnO}$  because of the lower nominal oxidation state.<sup>16</sup>

The numerically calculated single-particle electronic energy levels and their occupation for the band-structure-corrected calculation, as well as magnetic moments, are summarized in Fig. 2. Here, we show the nonbonding 3d level and the crystal field resonance (CFR). The dangling bond hybrid (DBH) is only shown for the special cases (denoted by an asterisk) when it lies inside the host band gap. The general trends in single-particle energy levels can be understood from the model in Fig. 1, recalling that the 3d orbital energies of the free atoms become deeper as the atomic number increases along the 3d row. For light 3d elements (Ti and V) the  $e(d)$  and  $t(d)$  energies are far above the anion dangling bonds, so the impurity interaction with the dangling bond is weak. For heavier 3d elements, the 3d energies and

TABLE II. On-site Coulomb corrections (in eV) for the transition-metal impurities.

$U_{\text{Sc } d}$	$U_{\text{Ti } d}$	$U_{\text{V } d}$	$U_{\text{Cr } d}$	$U_{\text{Mn } d}$	$U_{\text{Fe } d}$	$U_{\text{Co } d}$	$U_{\text{Ni } d}$	$U_{\text{Cu } d}$
1.8	2.0	2.3	2.6	3.9	3.5	2.8	3.4	6.0

anion dangling bonds become closer, leading to stronger interaction, and a larger crystal-field splitting. In addition, due to the lower oxidation state of the substitutional impurities in  $\text{ZnO}$ , the 3d levels, in general, lie at higher energies in  $\text{ZnO}$ . Table III summarizes the calculated spin configurations. Along increasing atomic number, both  $\text{ZnO}:3d$  and  $\text{In}_2\text{O}_3:3d$  exhibit a crossover from high-spin state to low-spin state around cobalt; that is, the crystal-field splitting exceeds the spin splitting. Co and Ni are the first low-spin elements in  $\text{In}_2\text{O}_3$  and  $\text{ZnO}$ , respectively. The crystal-field resonance in most cases is an antibonding level that lies above the host valence band. Only iron in  $\text{In}_2\text{O}_3$  forms an exception, exhibiting a dangling-bond hybrid inside the host band gap. In such cases, the hole is generally bound at one oxygen neighbor atom, which then assumes the nominal O(-I) oxidation state. While, experimentally, this behavior is well established for nontransition impurities, e.g., Al in  $\text{SiO}_2$  (Ref. 32) or Li in  $\text{ZnO}$ ,<sup>33</sup> density-functional calculations generally experience difficulties in correctly describing this hole localization due to residual self-interaction within the O  $p$  shell.<sup>34</sup> After an additional correction for localized hole states, such bound hole states tend to move deeper into the gap.<sup>35</sup>

For both carrier concentration and magnetic properties, it is important to take note of the position of the highest occupied 3d level [cf. highest occupied molecular orbital (HOMO)] with respect to the host band edges. For  $\text{In}_2\text{O}_3$ , this highest occupied level is always inside the host band gap, whereas for  $\text{ZnO}$ , Sc and Ti have occupied levels above the host conduction-band minimum (CBM). Notice also that, in general, all 3d defects that by simple electron counting would have a partially filled  $e$  or  $t$  gap level undergo a Jahn-Teller distortion, splitting the partially filled levels into fully occupied and empty levels [not observed in previous self-interaction-corrected coherent potential approximation (CPA) calculations<sup>36</sup>].

Figure 2 also illustrates the type of errors that would have resulted had we not fixed the correct relative energy positions of the host band edges and the 3d orbital energy. We calculated the same single-particle configurations also within the uncorrected generalized gradient approximation (GGA-PBE) functional, which underestimates the host oxide band gap by  $\sim 2$  eV. We see that using an uncorrected functional leads to some of the electrons that should reside on localized 3d gap levels to occupy lower-lying host conduction states instead. For example, the highest occupied Cr and Co levels in  $\text{ZnO}$  spill their electrons to conduction states in a GGA-PBE calculation, leading to a qualitatively incorrect description of magnetic interactions.<sup>19</sup> In terms of electronic doping, standard local-density approximations (LDAs) predict all 3d impurities to behave as shallow donors, which, as shown in the following, is not the case. This type of error

TABLE III. Electronic configurations corresponding to various “charge states” of transition-metal impurities in ZnO and In<sub>2</sub>O<sub>3</sub>. The transition energies  $\varepsilon(q/q')$  to change electronic configuration are given with respect to the valence-band edge  $\varepsilon_v$  in eV.

		In <sub>2</sub> O <sub>3</sub>							
		Ti	V	Cr	Mn	Fe	Co	Ni	Cu
$q=2-$							$t_{\pm}^6 e_{\pm}^2$		$t_{\pm}^6 e_{\pm}^4$
$\varepsilon(-/2-)$							3.35		2.51
$q=-$			$t_+^3$	$t_+^3 e_+^1$	$t_+^3 e_+^2$	$t_+^3 e_+^2 t_-^1$	$t_{\pm}^6 e_{\pm}^1$	$t_{\pm}^3 e_{\pm}^2$	$t_{\pm}^6 e_{\pm}^2 e_{\pm}^1$
$\varepsilon(0/-)$			3.36	4.00	2.04	0.79	2.74	0.79	1.49
$q=0$		$t_+^1$	$t_+^2$	$t_+^3$	$t_+^3 e_+^1$	$t_+^3 e_+^2$	$t_+^3 t_-^3$	$t_+^3 t_-^3 e_+^1$	$t_+^3 t_-^3 e_+^2$
$\varepsilon(+/0)$		2.70	1.61	0.29	1.26	0.77	0.15	0.41	-0.10
$q=+$		$t_+^0$	$t_+^1$	$t_+^2$	$t_+^3 e_+^0$	$t_+^3 e_+^2 + h$	$t_{\pm}^6 + h$	$t_{\pm}^6 e_+^0$	$t_{\pm}^6 e_+^1$
$\varepsilon(2+/+)$			0.49	-0.20		-0.12			
$q=2+$			$t_+^0$	$t_+^1$		$t_+^3 e_+^2 + 2h$			
		ZnO							
		Sc	Ti	V	Cr	Mn	Fe	Co	Ni
$q=-$								$e_+^2 t_+^3 e_-^2 t_-^1$	$e_{\pm}^4 t_{\pm}^3 t_{\pm}^2$
$\varepsilon(0/-)$								3.63	3.40
$q=0$		$e_+^1$	$e_+^2$	$e_+^2 t_+^1$	$e_+^2 t_+^2$	$e_+^2 t_+^3$	$e_+^2 t_+^3 e_-^1$	$e_+^2 t_+^3 e_-^2$	$e_{\pm}^4 t_{\pm}^3 t_{\pm}^1$
$\varepsilon(+/0)$		3.59	3.56	3.53	2.38	0.48	1.96	0.31	0.67
$q=+$		$e_+^0$	$e_+^1$	$e_+^2 t_+^0$	$e_+^2 t_+^1$	$e_+^2 t_+^2$	$e_+^2 t_+^3 e_-^0$	$e_+^2 t_+^3 e_-^1$	$e_{\pm}^4 t_{\pm}^3 t_{\pm}^0$
$\varepsilon(2+/+)$			2.05	0.64	0.77				
$q=2+$			$e_+^0$	$e_+^1$	$e_+^2 t_+^0$				

underlying both LDA or GGA and  $+U$  corrected functionals has caused significant confusion in the literature<sup>19,37,38</sup> as to the predicted magnetic behavior or conductivity. Here we rectify this problem by first applying a correction (see Sec. III) to the host crystal, recovering physically correct band-edge positions.<sup>19,20</sup> The  $3d$ -level position is further corrected by an on-site Coulomb  $+U$  term to account for the self-interaction correction. This combined host correction together with  $3d$  correction underlies all of our results below.

## V. DONOR AND ACCEPTOR TRANSITION ENERGIES

We obtain the transition energies  $\varepsilon(q'/q)$  as the direct evaluation via the total energies  $E(q)$  of the respective electronic configurations,

$$\varepsilon(q/q') = \frac{E(q') - E(q)}{q - q'} - E_v, \quad (1)$$

where  $q$  by convention denotes an electronic configuration, and  $E_v$  is the valence-band maximum. These transition energies for the  $3d$  impurities in In<sub>2</sub>O<sub>3</sub> and ZnO are given in Fig. 3 and Table II.

The general trend of the transition energies given in Fig. 3 emerges from the single-particle trends given in Fig. 2; that is, acceptor transitions are ensued by unoccupied single-particle levels, whereas occupied levels yield donor transitions. The acceptor transitions are somewhat higher in energy

than the unoccupied single-particle level that becomes occupied, and donor transitions lie at lower energies than the occupied single-particle levels that donate their electron to the conduction band. For high carrier concentrations we need a shallow donor type defect like Sn in In<sub>2</sub>O<sub>3</sub> and Al in ZnO.

The hallmark signature of shallow impurities is that their localized impurity states do not occur inside the gap, but as resonances inside the continuum of host states.<sup>39</sup> Thus, when such shallow donors are calculated in small supercells on the order of 100 atoms, corresponding to high impurity concentrations on the order of 1%, the introduced electrons are shed into the conduction band and raise the Fermi level above the CBM, due to the Moss-Burstein effect. As a result, the donor transition of shallow impurities is calculated inside the conduction band. While such band-filling effects can be corrected to deduce the transition level for the dilute doping limit,<sup>28,29</sup> both transparent conductors and ferromagnetic semiconductors require the incorporation of 1% or more impurity atoms. Therefore, rather than eliminating these band-filling effects, we here use the position of the calculated donor level inside the conduction band as an indicator for a shallow donor level as is the case for Sc, Ti, and V in ZnO [see Fig. 3(b)].

Some transition-metal impurities have a resonant state close above the CBM, which can lead to cause ferromagnetism when this state becomes occupied due to additional electron doping.<sup>19,20</sup> For example, the neutral Co<sub>Zn</sub>( $d^7$ ) impurity in ZnO does not possess an (0/-) acceptor transition inside the gap; i.e., when additional electrons are introduced

they first occupy the CBM rather than forming the charged  $\text{Co}_{\text{Zn}}^- (d^8)$  configuration. However, at very high levels of additional doping (e.g., by  $\text{Al}_{\text{Zn}}$ ), when the ensuing Moss-Burstein shift raises the Fermi level toward the empty  $d$  resonance inside conduction band, a partial occupation of the resonant Co state can be achieved.<sup>19,20</sup> Such a behavior, which is important for ferromagnetic wide-gap oxides (see below), is indicated when the  $3d$  impurity has a  $(0/-)$  transition close above the CBM, as is the case for V and Cr in  $\text{In}_2\text{O}_3$  [see Fig. 3(a)] and for Co and Ni in  $\text{ZnO}$  [see Fig. 3(b)].

$\text{In}_2\text{O}_3$  has the tendency to sustain more  $3d$  donor/acceptor transitions than  $\text{ZnO}$ . This evidences larger  $3d$ -O hybridization, accompanied with a smaller Mott-Hubbard  $U$  for the defect-host hybrid level.<sup>16</sup> The donor/acceptor transitions ensue a change of nominal oxidation state (reflected by a change in crystal-field resonance occupancy, as discussed in Ref. 16) for all transitions, with the exception of the donor transition induced by iron in  $\text{In}_2\text{O}_3$ . Here, the gap level that becomes unoccupied in fact is a dangling-bond hybrid, so before and after donor transition, the iron atom is nominally in the  $t_{+}^3 e_{+}^2$  configuration, and in the  $\text{Fe}^{3+}$  oxidation state.

As a consequence of (i)  $\text{In}_2\text{O}_3$  sustaining more donor/acceptor transitions and (ii) the higher-energy single-particle levels for  $3d$  impurities on  $\text{Zn}(+\text{II})$  sites than on  $\text{In}(+\text{III})$  sites, most transitions in  $\text{ZnO}$  are donors, while in  $\text{In}_2\text{O}_3$ , most  $3d$  impurities are amphoteric. Indeed, most  $3d$  impurities in  $\text{In}_2\text{O}_3$  have an acceptor transition in the upper part of the band gap (or right above the conduction-band minimum), which will act as a compensating center (killer-defect<sup>17</sup>) in the case of electron doping. Hence, due to the absence of shallow donors and the presence of electron killers, for  $\text{In}_2\text{O}_3$ ,  $3d$  doping will reduce carrier concentrations, as observed in experiment as an increase in resistivity of  $\text{In}_2\text{O}_3$  (or  $\text{In}_2\text{O}_3:\text{Sn}$ ) doped with Cr, Mn, Ni, and Cu.<sup>40,41</sup> On the other hand, experimentally doping of  $\text{In}_2\text{O}_3$  by Ti leads to degenerate electron doping.<sup>42,43</sup> In our calculation, Ti is indeed the only  $3d$  defect that does not behave as an electron killer (acceptor), so it allows an electron concentration without compensating for it. Our calculation of single defects, however, does not reveal the source of electrons, as the donor level due to Ti is too deep (CBM $-0.7$  eV) to produce a high concentration of electrons. Most likely the increase in free-electron concentration in Ti-doped  $\text{In}_2\text{O}_3$  samples is due to one of the following scenarios: (1) Ti forms some kind of clusters or complexes with, e.g., O (or intrinsic defects), which may alter the defect levels, as recently shown to be the case in cobalt-doped  $\text{ZnO}$ , where Co forms complexes with oxygen vacancies<sup>38</sup> (also, cf. cluster doping<sup>44</sup>); (2) precipitation of  $\text{TiO}_2$ ; (3) doping due to some unintentional defects; or (4) complex formation with some unintentional defects. With unintentional defects in (3) and (4) we imply some foreign defects attracted by the high electropositivity of Ti.

Due to the low oxidation state of the  $3d$  impurities substituting on the  $\text{Zn}(+\text{II})$  site, for  $\text{ZnO}$ , we predict Sc, Ti, and V to be shallow donors. Because the donor transition  $\varepsilon(+/0)$  for Sc, Ti, and V is essentially the same as that of Al, also the carrier concentrations have the same dependence on impurity concentration and growth environment (see Ref. 18). Indeed there are several experimental observations of

metalliclike electron conductivity induced by Ti doping of  $\text{ZnO}$ .<sup>45–49</sup> All the heavier  $3d$  impurities, like in  $\text{In}_2\text{O}_3$ , act as killer-defects and will reduce free-electron concentrations, as has been experimentally observed for, e.g., Mn (Ref. 50) doping of  $\text{ZnO}$ .

## VI. MAGNETISM

Figure 2 describes the magnetic state of isolated  $3d$  impurities. The knowledge of spin polarization of isolated impurities only indicates whether or not one can expect a paramagnetic response. For magnetization to persist in the absence of an external field, the  $3d$ - $3d$  impurity pairs must exhibit nonvanishing exchange interactions of sufficiently long range  $R > R_0$ , where  $R_0$  is the typical  $3d$ - $3d$  distance; i.e., the magnetic interaction forms a percolation path. Typically, ferromagnetic exchange interactions can only be expected for a single-particle configuration with partially filled levels,<sup>51</sup> unless there is an extraordinarily strong  $3d$ - $3d$  bonding interaction.<sup>52</sup> Neither the charge neutral nor any of the multiple charged configurations of the  $3d$  impurities in either host material have partially filled levels because of Jahn-Teller distortions, so partial occupancy of gap levels is unlikely to drive ferromagnetism. Instead, we have previously shown that even nondegenerate levels can be partially filled *if they are resonant inside the conduction band*.<sup>19,20</sup> Such states, even when strongly localized, are part of a continuum of states, and thus also their occupation number can be varied continuously.

For example,  $\text{Co}_{\text{Zn}}$  in  $\text{ZnO}$  introduces a  $t$  resonance about 0.5 eV above the CBM, and strong ferromagnetic Co-Co coupling occurs when this resonance becomes partially occupied upon additional electron doping.<sup>19</sup> However, due to the large energy separation between the Co  $t$  resonance and the CBM, there exists a threshold for the minimum electron concentration needed to instigate ferromagnetism: whereas a level of 1% doping, e.g., by  $\text{Al}_{\text{Zn}}$ , does not lead to significant magnetic Co-Co coupling, a higher doping level of 3% causes very strong FM interaction between close Co-Co pairs and still significant coupling for more distant pairs.<sup>19</sup> While such high levels of electron concentration may be not realistic [the doping limit lies at 1% (Ref. 9)], it was recently shown by Pemmaraju *et al.*<sup>38</sup> that the formation of a defect pair consisting of  $\text{Co}_{\text{Zn}}$  and a O vacancy lowers the energy of the Co  $t$  resonance, and thereby allows for FM coupling at lower electron concentrations. In Ref. 19, we found that Cr has an empty  $d$  resonance at only 0.2 eV above the CBM, leading to strong and long-range FM coupling already at the lower doping level of 1%. Thus Cr may not need the FM enhancing mechanism of pairing with O vacancies.

We further calculate the pairwise  $3d$ - $3d$  magnetic stabilization energies  $\Delta_{\text{FM}} = E_{\text{FM}} - E_{\text{AF}}$  from the total energies of ferromagnetic ( $E_{\text{FM}}$ ) and antiferromagnetic ( $E_{\text{AF}}$ ) configurations. Besides the above discussed cases of Cr in  $\text{In}_2\text{O}_3$  and  $\text{ZnO}$  and Co in  $\text{ZnO}$ , we consider Ti and Mn in  $\text{In}_2\text{O}_3$  in the absence of external carriers. Due to the lack of partially filled resonances, we only find weak-coupling energies ( $\Delta_{\text{FM}} > -15$  meV) with the exception of a Mn-Mn nearest-neighbor pair. For this Mn-Mn pair, we find  $\Delta_{\text{FM}} \sim -0.43$  eV, which

appears to be of the same type as the strong short-range interaction observed for Co-Co pairs in  $\text{Cu}_2\text{O}$  due to the formation of multiple direct  $3d$ - $3d$  chemical bonds.<sup>52</sup> This leads to the conclusion that, in general, partial occupancy is a prerequisite for ferromagnetic interactions,<sup>20,51</sup> unless direct chemical interactions overpower crystal-field or Jahn-Teller effects. Thus, long-range percolating ferromagnetic interactions can only be expected under extreme doping conditions, where the  $3d$  levels inside the conductance continuum of states become populated. Apart from extrinsic do-

nor doping, such conditions may be attained due to substantial structural imperfections. Interestingly, reports on  $3d$  ferromagnetism in ZnO stem mostly from structurally far-from-perfect samples,<sup>37</sup> while single-crystal samples are less likely to exhibit collective magnetism.<sup>53</sup>

#### ACKNOWLEDGMENT

This work was funded by DOE-EERE under Contract No. DE-AC36-08GO28308.

\*Present address: Department of Physics, Yokohama National University, Yokohama 240–8501, Japan. hannes@ynu.ac.jp

- <sup>1</sup>V. F. Masterov and B. E. Samorukov, *Sov. Phys. Semicond.* **12**, 363 (1977).
- <sup>2</sup>V. F. Masterov, *Sov. Phys. Semicond.* **18**, 1 (1984).
- <sup>3</sup>B. Clerjaud, *J. Phys. C* **18**, 3615 (1985).
- <sup>4</sup>A. Zunger, in *Solid State Physics*, edited by F. Seitz, D. Turnbull, and H. Ehrenreich (Academic, New York, 1986), Vol. 39, pp. 275–464.
- <sup>5</sup>D. S. McClure, in *Solid State Physics*, edited by F. Seitz and D. Turnbull (Academic, New York, 1959), Vol. 8, pp. 1–47.
- <sup>6</sup>D. S. McClure, in *Solid State Physics* (Ref. 5), Vol. 9, pp. 400–525.
- <sup>7</sup>G. Heiland, E. Mollwo, and F. Stöckmann, in *Solid State Physics* (Ref. 5), Vol. 8, pp. 191–323.
- <sup>8</sup>D. M. Smyth, *The Defect Chemistry of Metal Oxides* (Oxford University Press, Oxford, 2000).
- <sup>9</sup>H. L. Hartnagel, A. L. Dawar, A. K. Jain, and C. Jagadish, *Semiconducting Transparent Thin Films* (IOP, Bristol, 1995).
- <sup>10</sup>H. Munekata, H. Ohno, S. von Molnar, A. Segmuller, L. L. Chang, and L. Esaki, *Phys. Rev. Lett.* **63**, 1849 (1989).
- <sup>11</sup>H. Ohno, *Science* **281**, 951 (1998).
- <sup>12</sup>T. Dietl, H. Ohno, F. Matsukura, J. Cibert, and D. Ferrand, *Science* **287**, 1019 (2000).
- <sup>13</sup>M. Woodhouse, G. S. Herman, and B. A. Parkinson, *Chem. Mater.* **17**, 4318 (2005).
- <sup>14</sup>M. Woodhouse and B. A. Parkinson, *Chem. Mater.* **20**, 2495 (2008).
- <sup>15</sup>F. D. M. Haldane and P. W. Anderson, *Phys. Rev. B* **13**, 2553 (1976).
- <sup>16</sup>H. Raebiger, S. Lany, and A. Zunger, *Nature (London)* **453**, 763 (2008).
- <sup>17</sup>A. Zunger, *Appl. Phys. Lett.* **83**, 57 (2003).
- <sup>18</sup>S. Lany and A. Zunger, *Phys. Rev. Lett.* **98**, 045501 (2007).
- <sup>19</sup>S. Lany, H. Raebiger, and A. Zunger, *Phys. Rev. B* **77**, 241201(R) (2008).
- <sup>20</sup>H. Raebiger, S. Lany, and A. Zunger, *Phys. Rev. Lett.* **101**, 027203 (2008).
- <sup>21</sup>(a) V. I. Anisimov, J. Zaanen, and O. K. Andersen, *Phys. Rev. B* **44**, 943 (1991); (b) A. I. Liechtenstein, V. I. Anisimov, and J. Zaanen, *Phys. Rev. B* **52**, R5467 (1995).
- <sup>22</sup>G. Kresse and D. Joubert, *Phys. Rev. B* **59**, 1758 (1999).
- <sup>23</sup>P. Erhart, A. Klein, R. G. Egdell, and K. Albe, *Phys. Rev. B* **75**, 153205 (2007).
- <sup>24</sup>*Semiconductors: Data Handbook*, 3rd ed., edited by P. Madelung (Springer, Berlin, 2004).
- <sup>25</sup>M. Usuda, N. Hamada, T. Kotani, and M. van Schilfgaarde, *Phys. Rev. B* **66**, 125101 (2002).
- <sup>26</sup>S. Lany, J. Osorio-Guillen, and A. Zunger, *Phys. Rev. B* **75**, 241203(R) (2007).
- <sup>27</sup>The thermochemical determination of  $U$  (Ref. 26) becomes difficult for Ti and Sc, because the relative stability of different oxide stoichiometries depends weakly on  $U$ . The present values for Ti and Sc are estimated based on the trend that  $U$  becomes smaller towards the early  $3d$ 's, as the energies of the  $d$ -orbitals increase and their localization decreases. The conclusions of this work are not sensitive to the exact value of  $U$  for Ti and Sc.
- <sup>28</sup>C. Persson, Y. J. Zhao, S. Lany, and A. Zunger, *Phys. Rev. B* **72**, 035211 (2005).
- <sup>29</sup>S. Lany and A. Zunger, *Phys. Rev. B* **78**, 235104 (2008).
- <sup>30</sup>F. Oba, A. Togo, I. Tanaka, J. Paier, and G. Kresse, *Phys. Rev. B* **77**, 245202 (2008).
- <sup>31</sup>F. Sauberlich and A. Klein, *Compound Semiconductor Photovoltaics*, MRS Symposia Proceedings No. 763 (Materials Research Society, Pittsburgh, 2003), pp. 471–476.
- <sup>32</sup>M. C. M. O'Brien, *Proc. R. Soc. London, Ser. A* **231**, 404 (1955).
- <sup>33</sup>J. Schneider and O. F. Schirmer, *Z. Naturforsch. A* **18A**, 20 (1963).
- <sup>34</sup>J. Lægsgaard and K. Stokbro, *Phys. Rev. Lett.* **86**, 2834 (2001).
- <sup>35</sup>S. Lany and A. Zunger (unpublished).
- <sup>36</sup>M. Toyoda, H. Akai, K. Sato, and H. Katayama-Yoshida, *Physica B* **376-377**, 647 (2006).
- <sup>37</sup>J. M. D. Coey, *Curr. Opin. Solid State Mater. Sci.* **10**, 83 (2006).
- <sup>38</sup>C. D. Pemmaraju, R. Hanafin, T. Archer, H. B. Braun, and S. Sanvito, *Phys. Rev. B* **78**, 054428 (2008).
- <sup>39</sup>S. Lany and A. Zunger, *Phys. Rev. B* **72**, 035215 (2005).
- <sup>40</sup>J. Philip, A. Punnoose, B. I. Kim, K. M. Reddy, S. Layne, J. O. Holmes, B. Satpati, P. R. Leclair, T. S. Santos, and J. S. Moodera, *Nature Mater.* **5**, 298 (2006).
- <sup>41</sup>D. Bérardan, E. Guilmeau, and D. Pelloquin, *J. Magn. Magn. Mater.* **320**, 983 (2008).
- <sup>42</sup>A. E. Delahoy and S. Y. Guo, *J. Vac. Sci. Technol. A* **23**, 1215 (2005).
- <sup>43</sup>M. F. A. M. van Hest, M. S. Dabney, J. D. Perkins, D. S. Ginley, and M. P. Taylor, *Appl. Phys. Lett.* **87**, 032111 (2005).
- <sup>44</sup>L. G. Wang and A. Zunger, *Phys. Rev. B* **68**, 125211 (2003).
- <sup>45</sup>Y. R. Park and K. J. Kim, *Solid State Commun.* **123**, 147 (2002).
- <sup>46</sup>Y. M. Lu, C. M. Chang, S. I. Tsai, and T. S. Wey, *Thin Solid Films* **447-448**, 56 (2004).

- <sup>47</sup>S. S. Lin, J.-L. Huang, and P. Šajgalik, *Surf. Coat. Technol.* **191**, 286 (2005).
- <sup>48</sup>J. J. Lu, Y. M. Lu, S. I. Tsai, T. L. Hsiung, H. P. Wang, and L. Y. Jang, *Opt. Mater. (Amsterdam, Neth.)* **29**, 1548 (2007).
- <sup>49</sup>J.-L. Chung, J.-C. Chen, and C.-J. Tseng, *J. Phys. Chem. Solids* **69**, 535 (2008).
- <sup>50</sup>J. Han, P. Q. Mantas, and A. M. R. Senos, *J. Eur. Ceram. Soc.* **21**, 1883 (2000).
- <sup>51</sup>P. Mahadevan, A. Zunger, and D. D. Sarma, *Phys. Rev. Lett.* **93**, 177201 (2004).
- <sup>52</sup>H. Raebiger, S. Lany, and A. Zunger, *Phys. Rev. Lett.* **99**, 167203 (2007).
- <sup>53</sup>M. H. Kane, W. E. Fenwick, M. Strassburg, B. Nemeth, R. Varatharajan, Q. Song, D. J. Keeble, H. El-Mkami, G. M. Smith, Z. J. Zhang, J. Nause, C. J. Summers, and I. T. Ferguson, *Phys. Status Solidi A* **244**, 1462 (2007).